17th International Conference on Space Operations, Dubai, United Arab Emirates, 6 - 10 March 2023.

SpaceOps-2023, ID # 448

Aircraft Detection for Safe Optical Ground Station Operation

Andrea Di Mira[a]*, Julia Kirchner[b], Daniel Hampf[b], Nils Håkansson[b], Sven Bauer[b], Clemens Heese[a]

[a] *European Space Operation Centre, Robert-Bosch-Strasse 5, 64293 Darmstadt, Germany, andrea.di.mira@esa.int*
[b] *DiGOS Potsdam GmbH, Telegrafenberg 1, 14473 Potsdam, Germany, julia.kirchner@digos.eu*
* Corresponding Author

Abstract

Currently several networks of optical ground stations (OGS) are being planned and deployed for different space applications like commercial direct-to-Earth (DTE) optical communications, optical feeder links, satellite laser ranging and space debris collision avoidance services. To achieve their specific tasks, these stations typically uplink high-power non eye-safe laser beams across the sky. Laser beams can distract or injure pilots with temporary or permanent vision impairment and lead in the most critical cases to catastrophic events. This can pose serious threats to air traffic safety, when not addressed appropriately. This topic is highly relevant especially for the upcoming OGS networks which strongly benefit from autonomous operations without human presence for higher efficiency and quality of services. To this end a reliable system for aircraft detection deployed at each OGS is necessary to ensure safe operations and timely interruption of laser emission in case of predicted laser illumination of detected planes, helicopters and other manned flying objects. Transponder-based solutions offer a way for ground stations to monitor aircraft, but unfortunately today they cover only a part of the overall air traffic. In this paper a passive detection system based on multiple cameras operating in different spectral bands is presented. The detection algorithms developed make use of the collected images in the visible and different IR bands to identify laser beam-aircraft conjunctions and to automatically control OGS laser emission. An overview on the developed optical aircraft detection system and its performance will be presented. This technology complements existing methods of aircraft detection, offering broader coverage of monitorable targets and higher reliability to ensure safe OGS laser uplink operations.

Keywords: Aircraft Detection, In-sky Laser Safety, Infrared imaging.

Acronyms/Abbreviations

ADS-B	Automatic Dependent Surveillance-Broadcast
ADU	Aircraft Detection Unit
CNN	Convolutional Neural Network
CW	Continuous Wave
EBS	Event-Based Sensor
LEO	Low Earth Orbit
LMT	Laser Momentum Transfer
LWIR	Long-Wave Infrared
MPE	Maximum Permissible Exposure
MWIR	Mid-Wave Infrared
NOHD	Nominal Ocular Hazardous Distance
OGS	Optical Ground Station
SLR	Satellite Laser Ranging
SWIR	Short-Wave Infrared
TBAD	transponder-based aircraft detector
TIR	Thermal Infrared
VIS	Visible

1. Introduction

Several established and emerging applications for scientific or commercial purposes require the transmission of laser beams from ground to space through the atmosphere. Stations on ground with laser beam launching capability must implement measures not only for protecting operators from hazardous illumination inside and outside the station, but also for avoiding hazards to airplanes and other flying objects in the local airspace. Following are some examples of laser applications requiring attention to aircraft safety.

In satellite laser ranging (SLR) the range to satellites and their orbit characteristics is determined with high accuracy by measuring the time of flight of picoseconds laser pulses emitted from SLR stations on ground [1]. The average power emitted in this case may vary from few hundreds milliwatts for laser ranging to cooperative targets (i.e. satellites with retroreflectors) up to tens of watts for non-cooperative objects like rocket bodies, fragments and satellites parts not equipped with retroreflectors. The typical wavelength for SLR is 532 nm which, being in the visible spectrum, can be problematic for eye safety reasons. However, thanks to the increased availability of infrared detectors and the higher atmospheric transmittance, recent SLR implementations operate at 1064 nm (e.g. [2]) resulting in higher maximum permissible exposure (MPE) levels for eye and skin compared to visible laser light.

The use of lasers is exploited for telecommunications, thanks primarily to the intrinsic higher bandwidth provided by optical signals and lower power levels required for on-board satellite communications terminals. Optical communications have been studied for decades for high-rate satellite communications in LEO, lunar and deep space orbits. Most OGS architectures for optical communications include the uplink of a beacon laser to provide ground station angular position for supporting pointing acquisition and tracking of flying terminals. The emitted power levels and wavelengths depend primarily on the covered range and application. For example, in an optical LEO direct-to-Earth (DTE) communication scenario, 6 W average power at 1590 nm [3], while for deep space optical communications, ongoing experiments are based on multi-kW beacon source at 1064 nm [4].

High-power lasers have also been proposed for ground-based Laser Momentum Transfer (LMT), a future potential space debris mitigation strategy relying on small nudges applied via photon pressure to uncontrolled objects involved in detected conjunctions with active satellites in order to slightly perturb their orbits and allow timely collision avoidance. In such scenario the transmission of very high-power levels, up to 40 kW (continuous wave - CW) has been considered [5].

In astronomy lasers are used to create artificial guide stars for adaptive optics systems. They are usually pointed in areas of the sky where no sufficiently strong natural guide star is available to create a reference for the correction of atmospheric turbulence-induced wavefront errors [6]. This technology also finds application in future optical feeder links [7], which in turn employ kW-class lasers, as well as LMT ground stations [5].

Equal importance must be given to LIDAR systems for atmospheric remote sensing often emitting hazardous radiation levels.

Laser illuminations of flight crew personnel have occurred several times as documented in the examples provided in [8] resulting in aversion responses (e.g. blinking, squinting, head movement), temporary visual impairments, temporary visual loss as well as psychological effects. These reactions can obviously lead to catastrophic consequences and unfortunately illumination incidents still occur. For example, during 2021 pilots in the U.S. reported seeing lasers 9,723 times to the U.S. Federal Aviation Association [9].

Several regulatory efforts have been globally undertaken for the safe use of laser products. However, in the area of in-sky laser safety, regulations, guidelines and permission requests to local authorities for propagation of laser beams from optical ground stations is poorly harmonized and often considered a complicated matter. Nevertheless, it is essential that laser emission from these stations remains safe and does not endanger air traffic. This might require an operation concept allowing the interruption of laser transmission in presence of air traffic.

A robust aircraft detection system can highly support operations and the current transition to autonomous systems for future network of optical ground stations. To cope with clouds and weather effects strongly affecting link availability, ground stations diversity is envisioned, and several initiatives based on this concept have been launched for the development networks of optical ground stations ([10], [11]). These networks will require the capability of the stations to operate autonomously in an automated mode.

To ensure safe operations of laser-emitting stations, the European Space Agency recently launched an activity focusing on the implementation of a video-based real-time subsystem for detection of air traffic to be integrated in an OGS laser safety system with the objective to meet the in-sky laser safety requirements for autonomous and unmanned operations. This unit is based on passive optical detection and features multiple cameras sensitive in different spectral bands, visible and infrared. This paper reports on the progress of such development, conducted by the company DiGOS, and the ongoing system validation.

The first section provides an overview of the effects that may result from the propagation of lasers in the atmosphere and the international regulations developed in this area. A review of the main aircraft detection technologies is then conducted and an architecture for an OGS full laser safety system is introduced. In Sec. 2 the status of the ongoing multi-camera detection subsystem development is described with focus on the hardware components selected and the detection algorithms implemented. Finally, in Sec. 3 validation results and performance are discussed.

1.1 Laser Hazards for aviation and regulations

The principal concern for laser / aircraft interactions is the possibility for eye injuries to persons aboard the aircraft. A key figure is the Maximum Permissible Exposure (MPE). When the level of emitted power is above the MPE, laser illumination is considered to be hazardous up to a distance referred to as Nominal Ocular Hazardous Distance (NOHD). Both MPE and NOHD can be calculated according to the European standard EN 60825-1 [12], or the American ANSI Z136.1 [13]. These are determined by the wavelength, operation regime (single pulse, continuous wave, repetitively pulsed), laser power, time of exposure and possible use of optical aids. Beam divergence and emitting aperture are also important parameters for a laser safety assessment. MPE is also calculable for skin exposure, however these limits are significantly higher than for ocular hazard calculations. These factors are most important at the laser ground station itself, to protect personnel on site. Visual interference is also a major concern especially at lower altitudes, particularly for the possible effects on pilots' vison during critical phases of the flight such as take-off and landing. This refers to a bright light or distracting glare entering the cockpit, potentially causing interruptions to aircraft control. Visual interference is considered especially hazardous after dusk.

With the increasing occurrence of illumination incidents in the 1990s, regulations and standards were developed for outdoor laser use. In the US regulations (SAE AS 4970 [14]) have been developed in 1999 after the appearance of outdoor laser shows causing interference with air traffic. In 2000 the Safety Regulation Commission (SRC) conducted research activities for a European regulation framework related to aviation safety producing the EU SRC document No. 7 – 2000 [15]. However, since regulations differ a lot from country to country in the EU a generalization of safety regulatory requirements was not possible.

In 2003 a manual was published by the International Civil Aviation Organization (ICAO) with the contracting states being Canada, the Netherlands, the United Kingdom and the United States, as well as the Aerospace Medical Association and the International Federation of Airline Pilots Association [8]. The document covers mostly the same material as the SAE standard, while providing more info on the background (e.g. laser physics, biological effects of laser radiation, etc.), the distribution of various laser emission zone at airports and contains standardized sheets for notification of authorities of in-sky laser activities, including calculation guidelines for various relevant parameters.

With the Commission regulation No 1207/2011 issued on November 22nd 2011, all aircraft heavier than 5.7T or faster than 250kts became obliged to carry Automatic Dependent Surveillance-Broadcast (ADS-B, see Sec. 1.2) transponders within the EU. All affected aircraft had to be equipped with transponders working at 1090 MHz until June 7th 2020 [16]. There were attempts to have ADS-B transponders mandatory also on smaller or slower aircraft. However, this approach failed in 2017 upon the recommendation of the working group RMT.0679, which said that this extension would lead to an overload problem on the Mode-S frequencies, due to too many broadcasting transponders [17]. Consequently, not all aircraft are covered with ADS-B, in particular small aircraft passing by at low altitude and thus close at high velocities – e.g. an 8 m long Cessna 172, with a maximum altitude of 4 km at up to 300 km/h.

1.2 Aircraft Detection Systems

In general, an aircraft detection system for optical ground stations shall detect the presence of approaching flying objects and automatically terminate laser emission when the position of the aircraft is within a safety margin around the operational beam. Several methods have been developed over the years for detecting aircraft at laser-emitting sites. A simple but effective form of aircraft detection are human spotters visually monitoring air traffic in relation to the telescope mount orientation and beam projection angle to shut down laser systems when any aircraft approaching the laser beam is detected [18]. Even though spotters may intercept airplanes and other flying objects also in those circumstances in which other modern detection systems are prone to false alarms (imaging systems may interpret stars or birds as airplanes), they might not see through clouds or be distracted by other activities. Station operators might by supported by dedicated cameras, though this solution is not ideal for automated operations.

Radars are a reliable solution commonly in use for monitoring air traffic also at laser stations. This technology is based on two properties of radio waves, i.e. reflection and doppler effect used for the detection and speed measurement of aircraft [19]. The system described in [20] operates in X band and is slaved to the SLR telescope to detect aircraft within a cone around the transmitted laser beam. However, radars are active devices that could interfere with other radio-based systems. In co-located geodetic techniques, for example, Very Long Baseline Interferometry (VLBI) systems may not be able to tolerate the high power radiated by aircraft radars. [21]. Furthermore, beyond military applications for naval/terrestrial air surveillance, a custom solution might be required for adaptation to an OGS.

A way to overcome the problem of interference with existing radio infrastructure is based on the use of passive radar systems which operate without own active transmission, therefore not subject to licensing and not contributing to electromagnetic pollution. One or multiple sensors detect digital TV or radio signals (DVB-T, DAB) coming from the environment including those reflected from passing aircraft. The location of potential target is derived from the time-difference-of-arrival (TDOA) of direct and reflected echo signals. For example, the PARASOL system, based on this principle, has been proposed for switching on collision avoidance illumination of wind turbines when an aircraft appears [22]. Passive radar could prove an effective and low-cost detection for low-altitude aircraft in populated areas.

A well-established aircraft surveillance approach suitable also for ground station in-sky laser safety is based on reception of signals, transmitted from transponder-equipped aircraft, containing information about position determined via satellite navigation. The most widespread technology based on this concept is the Automatic Dependent Surveillance-Broadcast (ADS-B) system, periodically transmitting state vectors (position, velocity, identification) through Mode S Extended Squitter at 1090 MHz. The signals can be intercepted with an ADS-B receiver providing precise and real-time aircraft monitoring data to the receiving party. As these systems are inexpensive, easy to use, reliable in any kind of weather, they are operated by most commercial aircraft and have become standard installations in laser stations. Similarly, FLARM systems (portmanteau of 'Flight' and 'Alarm') rely on the transmission of GPS-based position information. In addition, each unit identifies its current phase of flight and calculates a forecast position accordingly. This predicted position also is transmitted by each FLARM unit. However, in contrast to ADS-B, FLARM's radio protocol is proprietary, and the signal strength of the message transmitted is much lower and it is transmitted on a concession-free radio frequency. Due to the low signal strength, typical detection ranges for the FLARM system vary between 3 km and 5 km, which is significantly lower than the detection ranges of other available methods. Due to its low costs and simplicity in operation FLARM has become a quasi-standard within the gliding community, also spreading to light airplane, ultra-light, helicopter, and aerial sports applications. Its threat detection algorithms are specifically designed to the requirements of sport aviation [23]. Additionally, a transponder-based aircraft detector (TBAD) has been developed and installed on several large astronomical telescopes to avoid aircraft illumination during laser guide star operations in use for adaptive optics systems [24]. This system detects transponder transmissions from aircraft at 1090 MHz in several formats including Mode-A and Mode-C responses to interrogations signals coming from ground facilities and other aircraft. TBAD is based on an array composed of seven narrow-band patch antennas. By evaluating the ratio of the array output to that of a single patch antenna, TBAD can ascertain if the source of transmission is within ~15° of the boresight direction. Some aircraft deliberately do not transmit their position in their transponder signal (e.g. military, police, some private jets). Multi-lateration (MLAT) increases the coverage, as it can locate aircraft which mask their position in the transponder signal. An MLAT system uses various receivers on the ground which determine an aircraft's position by time-of-flight differences of the transponder signal [25].

Optical systems can potentially extend air traffic detection coverage for safe laser operations. Cameras in conjunction with image processing algorithms have been used in laser-emitting stations as a passive technology for detecting aircraft or typical features of flying objects. Visible spectrum (VIS) cameras represent a highly available and cheap technology for detecting different types of objects in the sky including drones, clouds and airplanes [26]. This technology offers high spatial and temporal resolution with the possibility to have more details of the aircrafts or clouds in case of cloud imagers. However, their use is limited to daylight conditions and detection performance may be reduced in case of haze, smoke, fog, dust, aerosols due to the scattering effect associated to their presence in the atmosphere [27].

The infrared spectrum offers in general several advantages for passive detection thanks to the achievable high contrast between aircraft and background and longer range. In particular, the atmospheric transmission in the near infrared (NIR) and short-wave infrared (SWIR) regions - 0.7-1.0 μm and 1.0-1.7 μm respectively - is higher than in the visible band and target discrimination can be achieved with higher performance operating at these wavelengths [28]. The SWIR band has been shown to outperform both VIS and NIR in case of reduced atmospheric visibility and in particular in hazy, fog, smoke conditions offering stronger penetration [29]. Moreover, the signature of exhaust emissions of some aircraft in the mid-wave infrared (MWIR) spectrum around ~2 - 4.5 μm can be exploited for air traffic monitoring and detection [30]. However typical infrared imaging sensors have lower resolution and are not widely available or as developed as visible spectrum sensors. Measurements of heat radiation from targets in the long-

wave infrared (LWIR) i.e. from 8 to 14 μm can be easily achieved by imaging systems based on uncooled detectors which require less complex and more affordable design together with less maintenance. The SLR station at the Geodetic Observatory Wettzell has adopted aircraft detection system based on LWIR camera which show good aircraft detection rate with regard to Air traffic control (ATC), suitable for in-sky laser safety systems [31].

Visible or infrared cameras can have latencies up to few milliseconds. Other relevant technology inspired by biological vision are event-based cameras. These passive detection systems don't measure absolute brightness at constant rate, but asynchronously detect brightness changes at the time they occur, with latencies of micro to few nanoseconds. Each pixel works independently and without brightness changes, no output is generated, reducing redundant data and consequently transmission bandwidth [32]. This technology has potential to detect fast target motion with high dynamic range and have been used experimentally for observing space debris [33].

In addition to passive optical systems, there have been attempts in the SLR community to use active systems for aircraft and cloud detection. For example, in [34] an eye-safe LIDAR is presented capable of generating a ring projected laser beam enclosing the SLR laser for detection of air traffic within a cone around the beam.

To complete this review acoustic sensors are briefly introduced. Acoustic detection, used since World War I for aircraft detection, utilizes passive "listening" techniques. The presence and location of an aircraft is acquired by measuring typical acoustic pressure emitted by the engine of the flying target. Low-cost ground-based system consisting of set of microphones have been used to detect low-flying aircraft to a range of in the order of 10 km [35],[36]. The advantages and drawbacks of the most common detection sensors herein discussed are summarized in Table 1.

Table 1. Comparison of common aircraft detection methods and sensors

Detection	**Pros**	**Cons**
Human spotters	- Detection based on human senses - Less prone to false alarms	- Not suitable for automated OGS systems - Additional manpower required - Susceptible to distraction
Active Radars	- Accurate - Ability to cover long ranges	- Expensive, might require custom solutions - Might require approval from local authorities and can be subject to ITU regulations and restrictions.
Passive Radars	- Interference-free - Good performance in low altitude	- Low ranges achievable
Transponder-based systems	- Low cost - Accurate	- Not all aircraft are equipped with transponders
Visible cameras	- Low cost - Available in high number of pixels	- Limited performance in case of strong atmospheric scattering and presence of sun - Noisy for night-time operations - Visible features of clouds might induce false detection
IR cameras	- Detection independent from environmental visible light - Suitable for 24/7 operations	- more expensive compared to visible cameras - Limited number of pixels, lower resolution - thermal features of clouds might induce false detection

1.2 Architecture of OGS full laser safety system

One could conclude that for future robotic and autonomous optical ground stations, a laser safety system must rely on a combination of multiple sensor types for adequate probability of detection. In Figure 1 the architecture of a robust laser safety system for OGS is presented: the information gathered from multiple aircraft detection units (ADUs), independently surveying the sky, is sent to a central hub - the laser safety unit - which shuts off the laser in case any ADU signals an unsafe situation with limited latency via safety relay lines. The laser safety unit is also interfaced with a station protection unit which monitors overall station health, based on weather and internal environmental conditions, mains power, door switches, status of emergency stops, and triggers the interruption of laser emission in case of unsafe conditions for person inside and outside the station and for the station equipment. In Sec. 2 the multi-camera subsystem developed in the frame of an ESA project is presented. This passive optical ADU combines the output of different cameras and will serve as one fundamental element of a full laser safety system essential for the safe automated operation of laser-emitting ground stations.

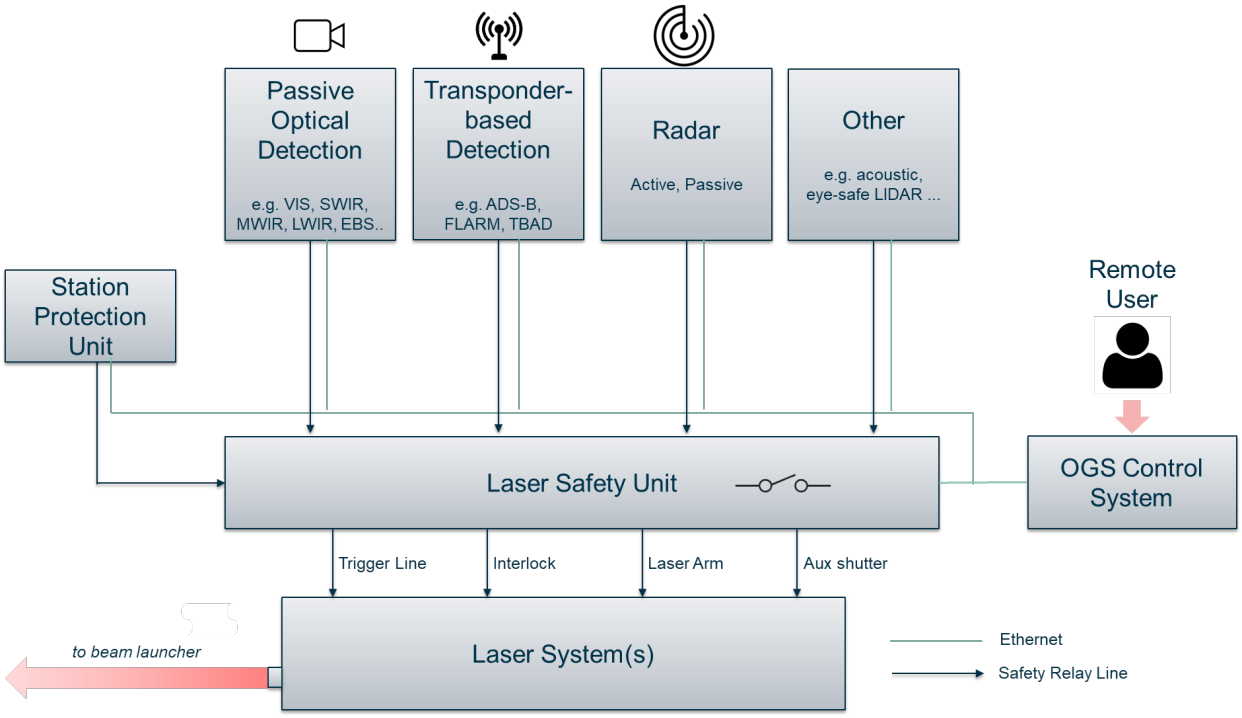

Fig. 1. OGS Robust aircraft detection system architecture

2. Multi-camera detection subsystem

Any safety system aiming at autonomous operation must guarantee to follow applicable regulations. During the design phase an extensive analysis of the requirements was undergone. The most relevant considerations are summarized in Sec. 2.1. Hardware and software decisions were made with those requirements in mind. Preliminary results are reported in Sec. 3.

2.1 Design considerations

2.1.1 Operational conditions

The detection system is designed for installation in laser ground stations that require a free line of sight to operate effectively. Heavily clouded and rainy conditions will generally mean a cessation of operations. Therefore, the safety system must operate nominally in clear skies, light haze or partly cloudy sky. A partly clouded sky may pose a special challenge, as aircraft may suddenly emerge behind clouds. Except for these adverse weather conditions, laser ground stations may work day and night, at any time of the week or year. Consequently, the same operational conditions apply for air-traffic safety. The same holds for temperature, wind and humidity limits to be expected at the station. For a video-based subsystem, the change in illumination conditions throughout the day / night cycle must be considered.

2.1.2 Maximum altitude and maximum distances

The Nominal Ocular Hazard Distance (NOHD) describes the distance at which a laser no longer presents a hazard to the human eye. Depending on the properties of the laser system, such as pulse energy, repetition rate and divergence, the NOHD can reach values well beyond 100 km. Such distances are hard to cover with almost any detection system and would potentially trigger false alerts. However, in practice it is usually sufficient to monitor a smaller distance range, if a minimum elevation is maintained in laser operations. Figure 2 shows the typical maximum flight altitudes of various types of air traffic, and the horizontal distance from the ground station to which they can be accidentally illuminated at given elevation angles. Even high-flying commercial aircraft are no longer endangered by laser installations beyond a ground distance of 40 km if a minimum elevation of 20° is used. More importantly, small and hard-to-detect aircraft are usually restricted to much lower altitudes, and thus are only relevant up to ground distances of 10÷15 km.

In rare cases, some air vehicles (e.g., fighter jets or scientific aircraft) might fly higher than 15 km. Even if they have a higher average speed than other air traffic, due to the high distance to the laser station, the angular speed can be low enough to enable successful and timely detection by the laser safety system. Also, they are usually large enough to still be detected (we assume a minimum size of 20 m).

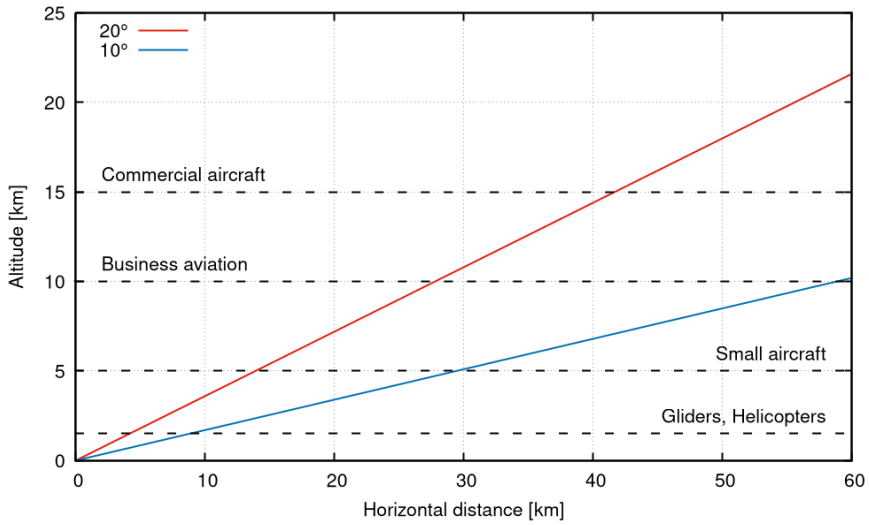

Fig. 2. Typical Maximum Altitude of Different Types of Air Traffic

2.1.3 Minimum altitudes and reaction times

The total reaction time must be fast enough to switch off the laser reliably before the aircraft gets near the laser beam. Figure 3 shows the angular speeds for typical aircraft operations versus distance from the laser ground station. Very high angular speeds exceeding 50°/s could be reached if a very fast aircraft would fly low over a station. However, this is not to be expected for most locations. Rather, low flying aircrafts will usually be either flying at reduced speed (e.g., commercial airliners in their starting / landing phase) or have inherently slower flying speeds (e.g., general aviation). Except during starting and landing, the lowest safe altitude in urban areas is defined as 300 m above the highest building or elevation in the vicinity, and 150 m outside urban areas [37]. The maximum angular velocity to be expected at 350 m distance is assumed to be 10°/s. At 2 km distance, the maximum angular velocity for commercial aircraft is about 3.5°/s.

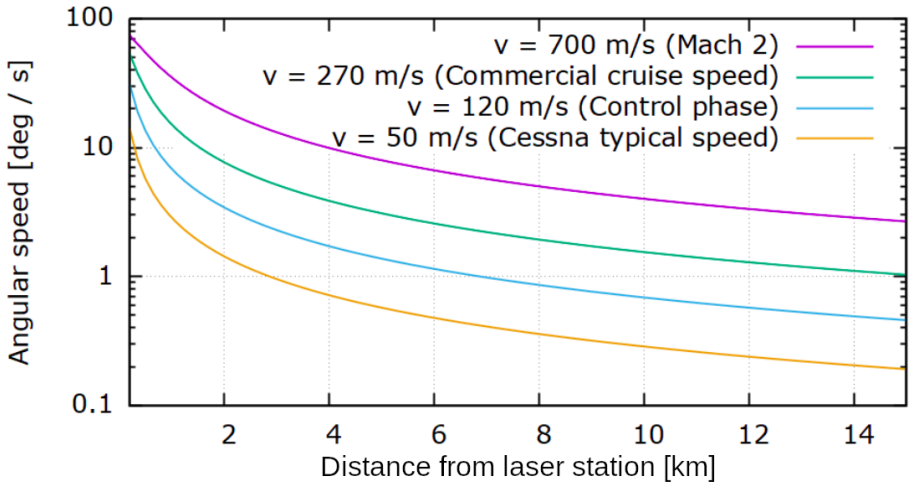

Fig. 3. Angular speeds versus distance to detection system, for typical aircraft operations. Control phase refers to landing / starting phases of commercial airliners.

2.2 Hardware

The hardware for this activity was chosen with respect to the considerations described in the previous section. Given the wide distance range to be covered, the system comprises cameras with varying FOVs. Three cameras with narrow FOV cover far-field detection of air traffic from 2 km and above. They are grouped in a compact camera unit that moves in line with the telescope. As mentioned in the previous section the maximum expected speed to be covered by the in-beam cameras is about 3.5°/s. An additional near-field camera with fixed mounting ("All-Sky" camera in the following) monitors the entire sky. Its main purpose is the detection of large, fast-moving objects moving up to 10°/s. Depending on the size of the objects, this camera covers distances from 0 up to 2 km. The most relevant specifications of all cameras are listed in Table 2. The SWIR camera was added for testing purposes to exploit detection in multiple IR spectral regions and is currently not integrated into the final system software.

Table 2. Selected cameras and their specifications

	Far-field TIR camera	**Far-field SWIR camera**	**Far-field VIS camera (monochrome)**	**Near-field VIS camera (colour)**
Model	Infratec VarioCAM HDx 625	Raptor Ninox 640	ZWO ASI 290MM	ZWO ASI 178MC
Resolution	640x480	640x512	1936x1096	3096x2080
Framerate	Up to 30 Hz	Up to 120 Hz	Up to 170 Hz	Up to 60 Hz
Field of View	10.4°x7.8° (with 60mm telephoto lens)	10.0° x 7.5° (with 50mm telephoto lens)	8.5 x 5.7° (with 40mm telephoto lens)	Entire sky

For system testing, a transportable mount was used. Figure 4(left) shows the validation setup with the mount and the camera unit on it. The All-Sky camera (Figure 4(right)) was placed separately. All images were recorded by a workstation in a movable rack. ADS-B signals were recorded in parallel using a Jetvision Radarcape receiver.

Fig. 4. Left: Validation mount with camera unit, right: All-Sky camera.

Figure 5 shows the architecture of the aircraft detection unit developed. While the camera unit is mounted on a movable tripod for system validation, the intended final installation is on the laser transmitter telescope of an OGS for routine operations. The All-Sky camera is placed independently, and an on-board Raspberry Pi handles the image acquisition. The remaining image acquisition is performed on the control PC, which also handles the image processing. Depending on the processing results, a relay is switched to control the laser interlock. Exchange of pointing information is enabled by a remote control interface. The mount publishes azimuth/elevation angles to a RESTful API and this information is read by the All-Sky camera to check whether objects are located into the region where the laser is transmitted.

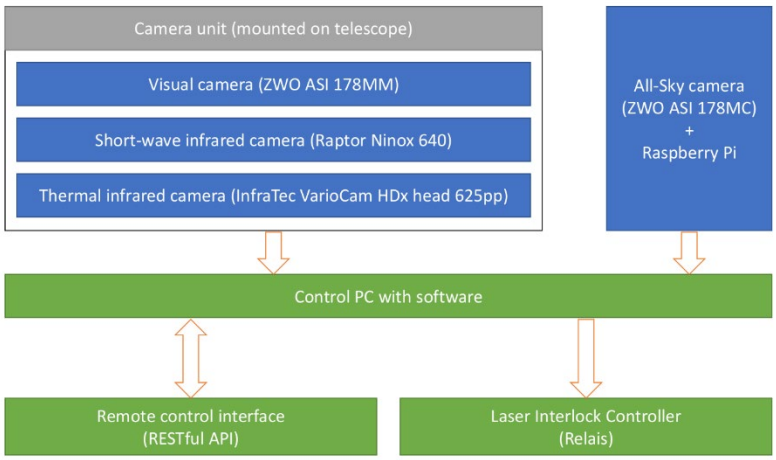

Fig. 5. Schematic of the multi-camera ADU.

2.3 Detection Algorithms

While the task of spotting aircraft in the sky is mostly trivial for human observers, the definition of decision rules is not straight-forward. Manned aircraft does not always look the same, depending on the kind of aircraft and the orientation and distance with respect to the camera. For example, at long distances, an aircraft might make up only a

few pixels within an image. In visible spectrum recordings, aircrafts could be the brightest or darkest feature, depending on their altitude and the position of the sun. Clouds could obscure them partially or completely or take over the role of the brightest feature. Some aircrafts show condensation trails while others do not. As the cameras follow the laser-beam, the recordings are non-static, thus an aircraft might seem to be motionless in consecutive frames.

The detection of in-sky aircraft has received growing attention in recent years. A binning algorithm incorporating thresholding in combination with edge detection has been presented by Wilkinson et al. [26]. The main drawback of the binning approach is its limitation to visible spectrum cameras and operations during daylight conditions. Due to the larger FOV of the used camera lens, the algorithm performance was not tested on distant, low-elevation aircraft.

A detection system based on convolutional neural networks (CNNs) has been created by Kashiyama et al. [38]. This algorithm requires visual images of high resolution and is limited to maximum distances of about 150 m. Because of this limitation, it might not be suitable for usage in a laser safety system. Another CNN-based algorithm operating on infrared images has been proposed by Wu et al. [39]. However, due to the need of clearly visible object features, machine learning techniques were so far not considered for the safety system design which requires detection of point-like objects in distances up to 40 km.

The algorithm for this activity was mainly inspired by the approach by Leidig et al. [31]. Their key similarity is the incorporation of the Canny edge detection algorithm. However, an additional processing step was included to enable detection for cameras in different wavelength regimes. The same algorithm is used for image processing on all camera streams simultaneously with different thresholds. The cameras selected have different number of pixels (cf. Table 2) and the processing time varies depending on image size. For the largest images (3096 x 2080) the processing time can be up to 180 ms. Figure 6 contains an example output for each of the processing steps introduced in the following.

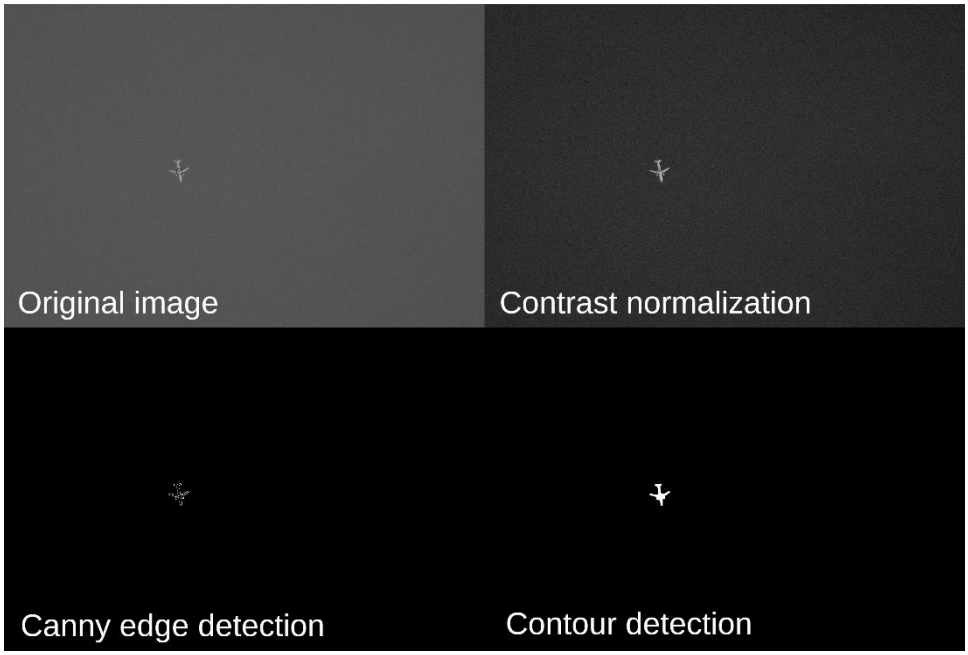

Fig. 6. Main processing steps of the detection algorithm for an example recording of the VIS camera.

Contrast normalization: VIS images often suffer from low contrast compared to those in the TIR regime. In order to highlight edges in the VIS images, the contrast needs to be increased. This is achieved by application of a min-max scaling that transforms the pixel intensities to the defined range of [0, 255]. The scaling also reduces differences resulting from varying lighting conditions and facilitates the usage of the same set of thresholds on all VIS images.

Canny edge detection: The Canny edge detection [40] is widely used in computer vision to find sharp intensity changes in an image. It classifies a pixel as an edge if the gradient magnitude of the pixel is larger than those of pixels at both its sides in the direction of maximum intensity change. The edge detection creates a binarized version of the image where pixels containing an edge are set to 1 and pixels without any edges to 0.

Contour detection: A closing operation is performed to merge close-by features which results in filled shapes. Contour detection [41] is then used to identify the locations of the shape's boundaries within the image. Given the contour, a bounding box is constructed around it. The algorithm finishes by returning the middle point of the bounding box.

2.4 Concept of operation

In each camera stream, a critical zone around the centre of the laser beam is defined. All detections within this zone are considered in the decision process for laser interruption. For safety, a diameter of 2.9° (half of the horizontal FOV of the VIS camera) was chosen initially. At the minimum distance of 2 km, an aircraft with the speed of 3.5°/s (Sec. 2.1.3) travels about 1.2° between two consecutive frames recorded at 3 Hz. Therefore, the system is configured to wait for two consecutive detection signals before shutting off the laser. The size of the critical area is the same for all cameras. To switch the laser back on again, a time span of 5 s (i.e., 15 frames at 3 Hz framerate) without any detections in the critical area are required. The size of the critical area depends on the time required for image capturing and processing as well as the fastest object to be detected.

3. Detection and validation results

About 24,000 images were recorded per camera for system validation. The presented results are based on three sessions in September and October 2022 covering day, twilight and night-time conditions for both clear-sky and sky with decent cloud coverage. The setup was placed on the rooftop near the Potsdam 3 Satellite Laser Ranging station on the Telegrafenberg in Potsdam, Germany. The height of the test site enabled the tracking of aircraft down to 15° elevation. Additional advantages of the Telegrafenberg are its proximity to the Berlin International Airport (about 40 km distance) and an airport in Trebbin (about 23 km distance) hosting small airplanes, gliders and balloons. Moreover, helicopters appear frequently in the region due to hospitals with dedicated landing places.

Manual alignment of the mount was required to maximize the amount of air traffic recorded in each session. The real-time aircraft tracking service Flightradar24 was used for indication where aircrafts might appear. Whenever an aircraft appeared in the sky, the cameras were pointed at it and the capturing was triggered. Mount positions and ADS-B signals were logged for evaluation.

3.1 Detection rates

For evaluation of the individual detection capabilities, the images of each camera were classified (aircraft/no aircraft) from the ADS-B logs using the image timestamp, pointing information and camera FOV. Images containing aircraft according to the ADS-B records were processed and evaluated by the object detection algorithm. Any image flagged by both the ADS-B and the video-based subsystem was considered a successful detection. Most images were recorded in clear sky conditions or with high-altitude clouds in the background. In some cases, low-altitude clouds with sharper defined edges raised false positives. For the scope of this activity, the occurrence of false positives due to dense clouds is considered acceptable, given that such scenario prevents laser operations, anyway. Additionally, aircraft can potentially emerge behind a dense cloud at any time. Thus, their presence near the laser beam also requires laser shut-off.

The detection rates additionally depend on the position of the aircraft relative to the observing system. Figure 7 shows the daytime single-frame detection rates of all cameras for clear-sky and cloudy background with respect to distance and elevation. The histograms contain the distribution of tracked aircraft over distance and elevation. They were obtained using the image timestamp, the corresponding mount position and ADS-B records matching both the timestamp and the pointing. From the ADS-B records, the position and distance of the aircraft in the image could be derived. The average detection rate of the VIS camera is between 70% and 90%, with a decrease towards high distances and low elevations. A high, nearly constant trend is observed in the SWIR, however, its high sensitivity for clouds (see Sec. 3.2) is skewing the results. The TIR shows a clear drop in the detection rate for distances higher than 25 km and elevations below 30°. A likely cause is that the atmospheric layer is much thicker at low elevation angles making it quite hard for the TIR camera to capture the heat signatures of distant objects.

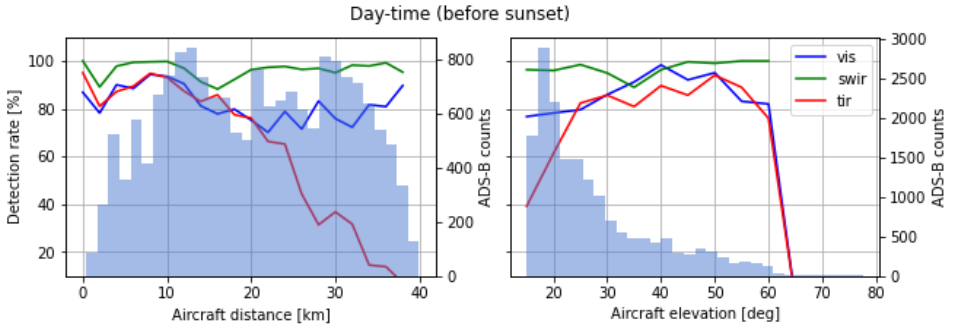

Fig. 7. Single-camera detection rates and aircraft distribution over aircraft distance and elevation during daytime.

A similar behaviour is present in the TIR night-time detection rates (see Figure 8). However, the TIR camera detects objects with higher reliability compared to the VIS cameras in almost all night-time scenarios. Given its independence of light, the TIR can detect aircraft without the need of sunlight or artificial lighting. In the VIS regime, the airplanes are visible only with anti-collision light turned on. Night-time recordings of the SWIR camera were not available at the time of writing this paper.

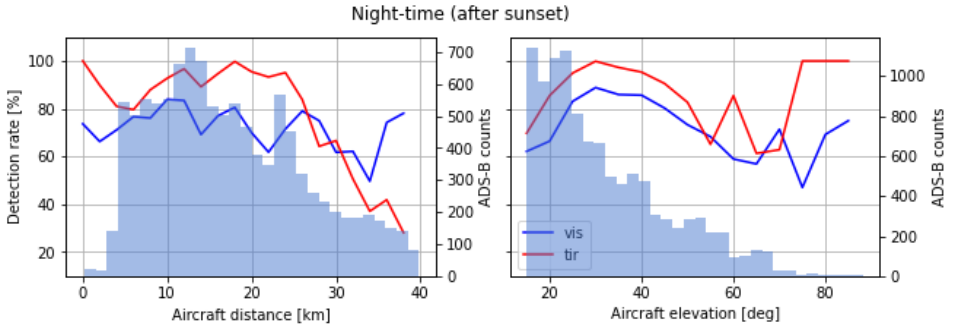

Fig. 8. Single-camera detection rates and aircraft distribution over aircraft distance and elevation during night-time.

These preliminary single-frame detection rates can only serve as indicators for two reasons. First, the test set contains some cases where the aircraft had just left the frame and its position was still close to the mount position, thus issuing an incorrect label. Another influence is the number of available test data. The distributions of tracked aircraft in the histograms indicate that most records cover medium distances and low elevations. Particularly low-distance and high-elevation aircraft is hardly present in the test set, such that the corresponding detection rates are more error prone. The overall video-based subsystem performance is discussed in Sec. 3.4.

3.2 Camera comparison: Case studies

The advantage of the multi-camera detection subsystem is its capability to compensate the weaknesses of a single camera. Usually, night-time operation is the typical use-case for preference of the TIR result over the VIS result. However, rare cases of VIS detection failure might be observed at daytime as well. Figure 9 shows the VIS (left) and TIR recording (right) of a close-by aircraft at about 6 pm local time, shortly before sunset. At low sun elevations, only high-altitude objects can reflect enough light to stand out in the VIS regime. The TIR sensor, on the other hand, captures the infrared radiation emitted by the surface such that the airplane clearly stands out.

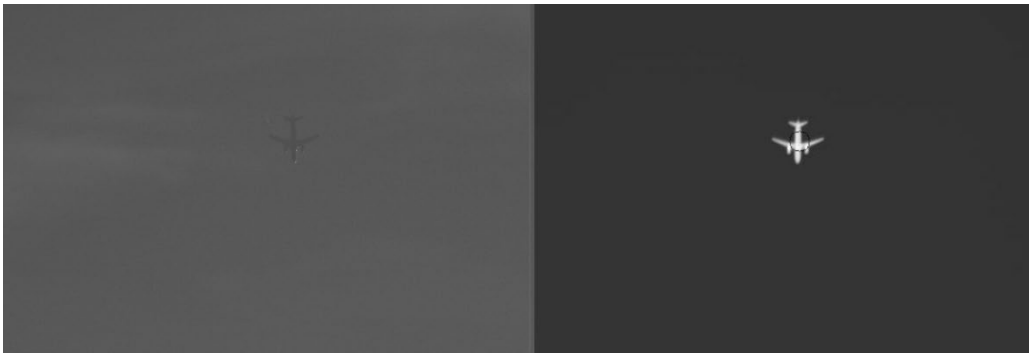

Fig. 9. Low-altitude aircraft just before sunset as seen by the VIS (left) and TIR (right) camera.

Another critical situation of an aircraft flying at 18° elevation at a distance of 34 km is shown in Figure 10. Due to the thick, warm atmosphere, the aircraft is hardly visible in the TIR camera (right) and does not get detected. In the VIS spectrum (left) detection is possible due to the condensation trail.

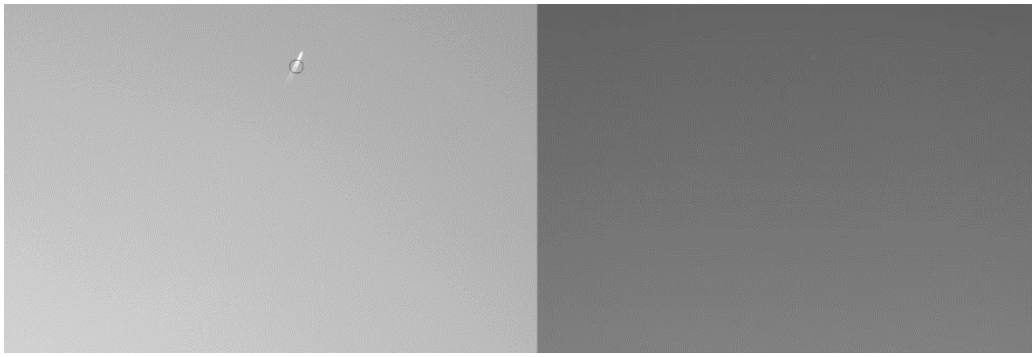

Fig. 10. Distant, low-elevation aircraft during daytime as seen by the VIS (left) and TIR (right) camera.

Figure 11 shows the same aircraft at 18° elevation with cloudy background recorded in all three cameras (from left to right: VIS, SWIR, TIR). While the aircraft is an outstanding feature in the VIS and the TIR recordings, it is hardly visible in the SWIR regime making it more difficult for the algorithm to detect. On the other hand, the diffuse clouds are most prominent in the SWIR recordings due to their high contrast compared to the background. In the VIS, the clouds are mostly visible, but not as clear. The TIR image contains only a small fraction of the clouds, and their borders appear less prominent than in the other images. For object detection, this scenario shows the advantages of the VIS and TIR wavelength regimes as the aircraft is best visible and false alarms resulting from clouds are minimized. However, the SWIR could be considered in the future for cloud detection.

Fig. 11. Example of an aircraft recorded in the presence of clouds as seen by the VIS (left), SWIR (middle) and TIR (right) camera.

3.3 Detection of low-altitude aircraft

In-time detection of fast, low-flying aircraft in the All-Sky camera has undergone initial testing, but so far, no systematic tests were possible due to a low number of close-by aircrafts. An example recording of a low-flying aircraft in the All-Sky camera is shown in Figure 12. An Airbus A319 was flying at about 2 km distance relative to the test setup. Regardless of its proximity, the airplane appears only in the size of a few pixels. The image processing algorithm for the All-Sky camera is being currently fine-tuned.

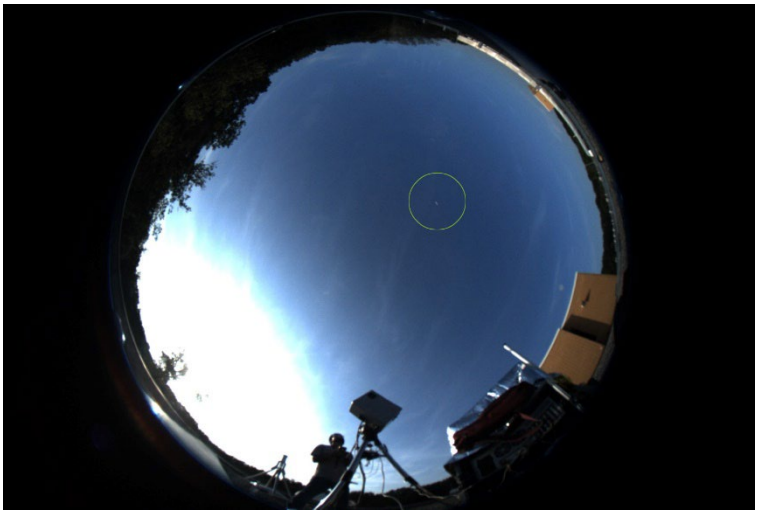

Fig. 12. Example of low-distance Airbus A319 as seen by the All-Sky camera.

3.4 System performance

In the following, a false alarm is defined as an erroneous detection in the absence of any object (not only aircraft). For the purpose of this activity, detections originating from clouds are not declared false alarms as aircraft could emerge behind them at any time. Similarly, to safeguard birds, the OGS laser must be switched off in case of detections in a region around the beam. Therefore, bird detections are not considered false alarms. What the term does cover are wrong detections, e.g., due to gradients in the sky lighting or temperature as well as stars. To estimate the false-positive rate, about 5,000 clear sky images without any objects were recorded for different pointing directions, i.e., including proximity to the sun and low elevations. The dataset contains night-time recordings as well. All images of each camera were processed by the detection algorithm with the result that no events falling into this definition of false alarm were reported.

For characterization of the multi-camera subsystem performance, aircraft recorded by the VIS and TIR in-beam cameras in parallel was considered. The SWIR is excluded from this analysis as it is currently not integrated into the system software. For each timestamp, the output of the processing algorithms (aircraft/no aircraft) was stored together with the timestamp. As discussed in Sec. 2.4, detections from previous frames are also considered. If any of the cameras successfully detected the object in the actual or one of the fourteen previous recordings, the aircraft is considered to be successfully detected as no illumination could take place.

The detection rates for the combined system with respect to aircraft distance and elevation are depicted in Figure 13. The histograms show the aircraft distribution on which the detection rates were computed. Considering both cameras and the previous recordings, the detection rate of the combined system reaches a total detection rate of 98% during daytime and 97% at night over all distances and elevations. Missing detections are reported mainly at higher distances above 22 km. An outlier analysis reveals that those undetected frames often don’t contain aircraft and were just recorded with the mount pointing close to a potential aircraft position.

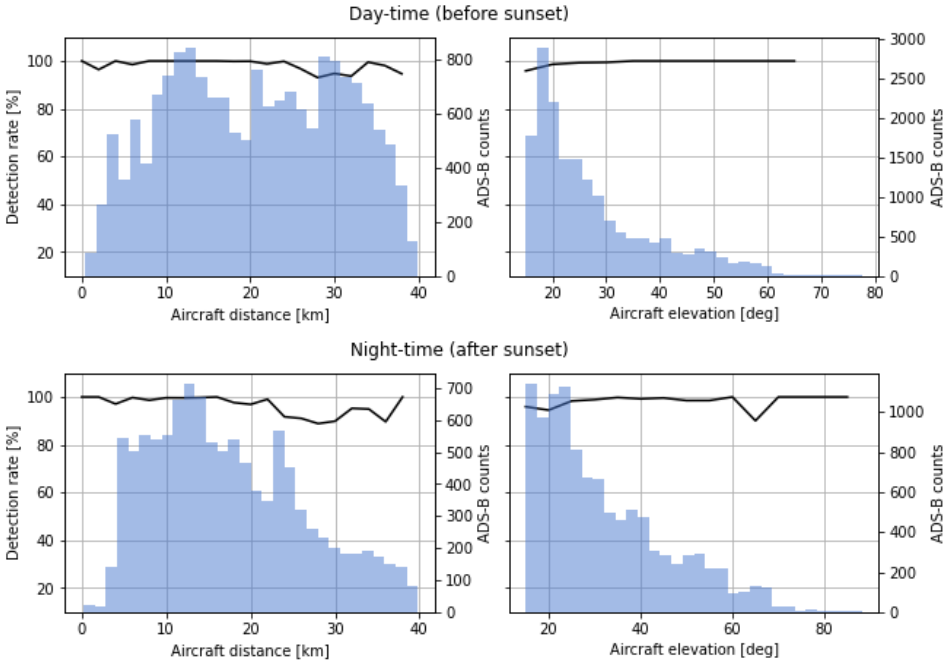

Fig. 13. Detection rate and aircraft distribution of the combined system over aircraft distance and elevation during daytime (top) and night-time (bottom).

3.5 Aircraft without ADS-B signature

Some of the aircraft spotted during the validation sessions did not appear in Flightradar24. On the chosen test site these cases were rare compared to the ADS-B equipped flights. Nevertheless, about 200 frames containing 3 airplanes without ADS-B signal were captured. An example is shown in Figure 14 for the VIS (left) and the TIR camera (right).

Fig. 14. Example of an aircraft without ADS-B signature as seen by the VIS (left) and TIR (right) camera.

In one case, an unknown object without ADS-B signature was raising at low elevation above the Telegrafenberg (distance about 500 m with respect to the test site). Figure 15 contains the corresponding magnified recordings (from left to right: VIS, SWIR, TIR). Due to its slow falling dynamics like a parachute, the object is assumed to be a weather balloon. In all cameras, the object was successfully detected.

Collection of more validation images containing different kinds of flying objects would further highlight the advantages of the video-based subsystem.

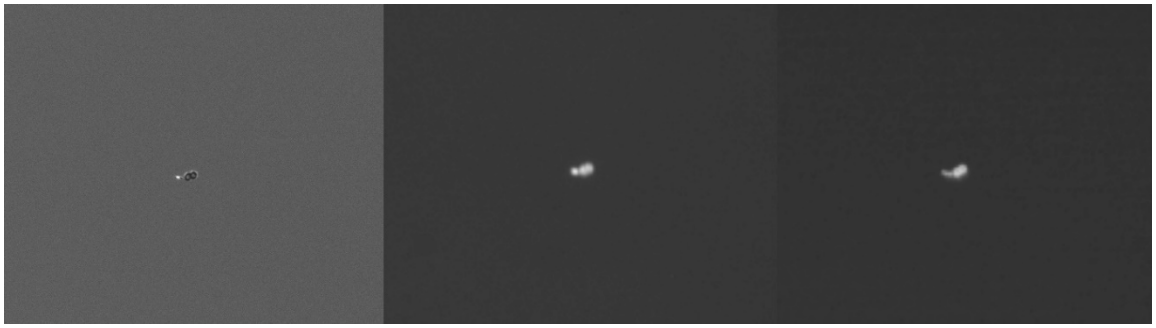

Fig. 15. Example of an unknown object, presumably a weather balloon, without ADS-B signature as seen by the VIS (left), SWIR (middle) and TIR (right) camera.

3.6 Possible improvements and outlook

Detection capabilities are mostly limited by the object's visibility in each wavelength regime. Whenever an aircraft is visible in the frame by eye, the algorithm has proven to efficiently detect it. Critical cases highlighted previously are usually covered by utilizing multiple cameras. Higher detection rates can potentially be achieved by setting lower thresholds during the edge detection process. However, this will result in an increasing number of false positives. A possible improvement to aircraft localization could be the analysis of condensation trails present in VIS and SWIR recordings. Currently, proximity of an airplane and its trail might potentially result in the identification as a single, large contour. As the position is determined from the centre of the contour, the algorithm might predict the airplane within its trail rather than at the tip of it (see Figure 16). Possible extensions of the current algorithm could include line detection, e.g., using the Hough transformation algorithm [42]. After extracting the most prominent lines in the image, a triangle could be fit with its tip most likely being the aircraft location. Alternatively, the usage of CNNs or other machine learning models for the dedicated task of identifying aircraft in the presence of condensation trails is imaginable.

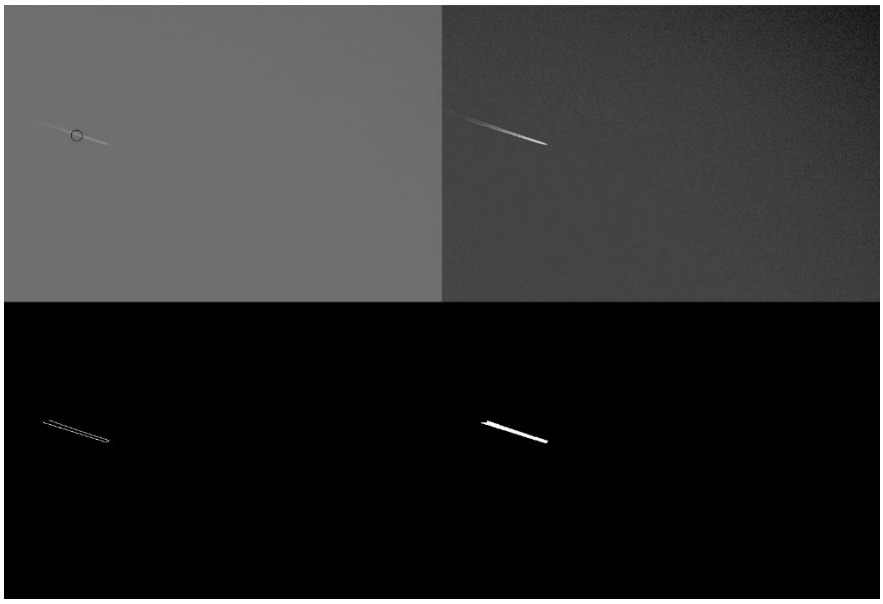

Fig. 16. Processing steps of the detection algorithm for an example recording of the VIS camera. The aircraft currently gets detected within the condensation trail instead at the front of it.

While false positives originating from low-altitude clouds are mostly unproblematic for laser operations, they nevertheless influence aircraft detection rate estimates for cloudy conditions. In the future, additional cloud detection algorithms could provide more precise estimates. The system will be further validated with possible improvements in the estimate of detection rates particularly for the All-Sky camera. Additional object detection algorithms, such as blob detection, will be tested.

4. Conclusions

This paper presents a video-based subsystem based on multiple cameras for reliable detection of air traffic during optical ground stations operations. This unit is a key element for safe control of laser emission and is intended to integrate the safety measures and devices that are part of a laser station, being used for laser ranging, optical communications, space debris remediation or for any other scientific purposes. Different cameras in the visible SWIR and thermal infrared have been integrated in a single unit that, mounted on the laser transmitting telescope, is capable of detecting objects in the direction of the beam and triggering laser switch off when air traffic is approaching the sky region illuminated by the laser. An all-sky camera complements the system providing a wide angle sky surveillance for near-field fast-moving objects. The algorithm implemented is based on Canny edge detection and is used simultaneously for all cameras.

While the project is still ongoing, its value for autonomous laser operations has been highlighted. Initial estimates of the single-camera detection capabilities were presented for varying scenarios and underlined in case studies. For the first time, SWIR recordings were considered for in-sky aircraft detection for optical ground stations. While this wavelength regime did not aid the detection of aircraft so far, a potential advantage for cloud detection was identified. Finally, the detection capability of the combined system was estimated to lie between 97% to 98% on average, and a more detailed correlation to aircraft position and lighting conditions was presented. Several detections of objects without ADS-B signature have been possible with the developed setup, proving the importance of complementing OGS in-sky laser safety measures with the presented detection unit for flying targets not equipped with transponder. Possible algorithm extensions have been identified based on line detection for handling condensation trails. Future machine learning techniques could be explored for increased performance. Plans are being made for field validation at an existing optical ground station.

Acknowledgments

The authors would like to thank ESA TDE programme for funding the activity and DiGOS team for the helpful discussions which led to the promising results presented in this work. The authors would like to acknowledge the support of the TEC-MME team at ESTEC for their help with the SWIR camera.

References

[1] M.R. Pearlman, J.J. Degnan, J.M. Bosworth, “The International Laser Ranging Service”, Advances in Space Research, Volume 30, Issue 2, 2002.

[2] A. Kloth, J. Steinborn, J. Munder, I. Zayer, G. Kirchner, S. Salmins and T. Schildknecht, “Towards Turnkey SLR Systems: New ESA Laser Ranging Station (ELRS),” in 21st International Workshop on Laser Ranging, Canberra, Australia, 2018.

[3] S. Alam, A. Di Mira, M. Yarrow, C. Heese, J. Singleton, A. Kloth, S. Steinborn and J. Clowes, “Beacon system for ESA IZN-1 Optical Ground Station,” in IEEE International Conference on Space Optical Systems and Applications (ICSOS), Virtual, 2022.

[4] A. Biswas, M. Srinivasan, S. Piazzolla, and D. Hoppe "Deep space optical communications", Proc. SPIE 10524, Free-Space Laser Communication and Atmospheric Propagation XXX, 2018

[5] S. Scharring, H. Dreyer, G. Wagner, J. Kästel, P. Wagner, E. Schafer, W. Riede, C. Bamann, U. Hugentobler, P. Lejba, T. Suchodolski, E. Döberl, D. Weinzinger, W. Promper, T. Glohrer, S. Setty, I. Zayer, A. Di Mira, E. Cordelli, “LARAMOTIONS: a conceptual study on laser networks for near-term collision avoidance for space debris in the low Earth orbit”, Appl. Opt., 60 (31), 2021.

[6] N. Ageorges and C. Dainty, "Laser guide star adaptive optics for astronomy," in Series C: Mathematical and physical sciences, vol 551, Springer, 2000.

[7] N. Védrenne, J. -M. Conan, A. Bonnefois, C. Petit, M. -T. Velluet and V. Michau, "Adaptive optics pre-compensation for GEO feeder links: Towards an experimental demonstration," 2017 IEEE International Conference on Space Optical Systems and Applications (ICSOS), Naha, Japan, 2017.

[8] International Civil Aviation Organization (ICAO), "Manual On Laser Emitters and Flight Safety", DOC 9815, AN/447, 2003.

[9] https://www.laserpointersafety.com/

[10] M. Krynitz, C. Heese, M. Knopp, K. J. Schulz and H. Henniger, "The European Optical Nucleus Network," 16th International Conference on Space Operations (SpaceOps 2021), Cape Town, South Africa, 2021.

[11] F. Bennet, K. Ferguson, K. Grant, E. Kruzins, N. Rattenbury, and S. Schediwy "An Australia/New Zealand optical communications ground station network for next generation satellite communications", Proc. SPIE 11272, Free-Space Laser Communications XXXII, 1127202 (2 March 2020)

[12] DIN e.V., "Safety of laser products - Part 1: Equipment classification and requirements; German and English version EN 60825-1:2014/prAA:2019", Beuth-Verlag, Berlin, 2019.

[13] ANSI Standard Z136.1 2014. American National Standard for the Safe Use of Lasers

[14] SAE Standard AS4970: Human Factor Considerations for Outdoor Laser Operations in the Navigable Airspace. Society of Automotive Engineers, Warrendale (PA), 2011. https://www.sae.org/standards/content/as4970/

[15] "COMMISSION IMPLEMENTING REGULATION (EU) No 923/2012 of 26 September 2021 laying down the common rules of the air and operational provisions regarding services and procedures in air navigation and amending Implementing Regulation (EU) No 1035/2011 and Regulations (EC) No 1265/2007, (EC) No 1794/2006, (EC) No 730/2006, (EC) No 1033/2006 and (EU) No 255/2010", https://eur-lex.europa.eu/eli/reg_impl/2012/923/2017-10-12

[16] European Organisation for the Safety of Air Navigation, "COMMISSION IMPLEMENTING REGULATION (EU) No 1207/2011", http://data.europa.eu/eli/reg_impl/2011/1207/2017-03-27, November 22nd 2011.

[17] Dr. Michael Erb, "Die Zukunft von ADS-B in Europa", in: AOPA Germany, https://aopa.de/2019/04/04/die-zukunft-von-ads-b-in-europa/, April 4th 2019.

[18] G. Rahmer, M. Lefebvre, and J. Christou, Julian "Aircraft safety and operational efficiency during LGS operations at the Large Binocular Telescope Observatory", Adaptive Optics for Extremely Large Telescopes AO4ELT5, 2017.

[19] M. I. Skolnik. "Radar Handbook (3rd ed.)", McGraw-Hill, 2008.

[20] J. F. McGarry, E. D. Hoffman, J. J. Degnan, J. W. Cheek, C. B. Clarke, I. F. Diegel, H. L. Donovan, J. E. Horvath, M. Marzouk, A. R. Nelson, D. S. Patterson, R. L. Ricklefs, M. D. Shappirio, S. L. Wetzel, and T. W. Zagwodzki, "NASA's satellite laser ranging systems for the 21st century," J Geod. 93, 2249–2262 (2018).

[21] C. Beaudoin, B. Corey, L. Hilliard, B. Petrachenko, "RF Compatibility of VLBI with DORIS and SLR at GGOS Stations: an Experimental Methodology to Validate the Models", IVS 2012 General Meeting Proceedings

[22] J. Heckenbach, H. Kuschel, J. Schell and M. Ummenhofer, "Passive radar based control of wind turbine collision warning for air traffic PARASOL," 2015 16th International Radar Symposium (IRS), Dresden, Germany, 2015.

[23] C. G. Santel, U. Klingauf, "A Review of Low-Cost Collision Alerting Systems and their HMIs", Technical Soaring, 2012.

[24] T. W. Murphy, “A Transponder-Based Aircraft Detector for SLR”, 19th International Workshop on Laser Ranging, Annapolis, 2014.

[25] H. Glaser-Opitz, J. Labun, “Means of integrating MLAT and ADS-B in up to date surveillance systems”, Proceedings of the International Scientific Conference New Trends in Aviation Development, 2014.

[26] M. Wilkinson, "Optically Detecting Aircraft for In-Sky Safety in Daylight Conditions", NERC Space Geodesy Facility, Herstmonceux, UK, ILRS Technical Workshop, Stuttgart 2019.

[27] Wang Y, Liu D, Xie W, Yang M, Gao Z, Ling X, Huang Y, Li C, Liu Y, Xia Y. “Day and Night Clouds Detection Using a Thermal-Infrared All-Sky-View Camera”. Remote Sensing. 2021.

[28] Lindsey Wiley, Joshua Follansbee, Patrick Leslie, Orges Furxhi, Rich Pimpinella, David Brady, and Ronald Driggers "Target discrimination in the extended SWIR (eSWIR) band (2-2.5μm) compared to Vis, NIR, and SWIR in degraded visual environments", Proc. SPIE 12106, Infrared Imaging Systems: Design, Analysis, Modeling, and Testing XXXIII, 1210606 (27 May 2022).

[29] R. G. Driggers, V. Hodgkin, R. Vollmerhausen, "What good is SWIR? Passive day comparison of VIS, NIR, and SWIR", Proc. SPIE 8706, Infrared Imaging Systems (2013).

[30] Jack R. White, “Aircraft Infrared Principles, Signatures, Threats, and Countermeasures”, Naval Air Warfare Center Weapons Division, 2012.

[31] A. Leidig, U. Schreiber, T. Bachem, M. Hohlneicher, G. Herold, S. Mähler, C. Schade, O. Lang, J. Eckl, S. Riepl, A. Böer, "Free Space Laser Safety System for Aircraft Camera Detection in the Infrared", Geodetic Observatory Wettzell, ILRS Technical Workshop, Stuttgart 2019.

[32] G. Gallego, T. Delbruck, G. Orchard, C. Bartolozzi, B. Taba, A. Censi, S. Leutenegger, A.J. Davison, J. Conradt, K. Daniilidis, et al. “Event-Based Vision: A Survey”, IEEE Trans. Pattern Anal. Mach. Intell. 2022.

[33] G. Cohen, S. Afshar, A. van Schaik, A. Wabnitz, T. Bessell, M. Rut-ten, and B. Morreale, “Event-based sensing for space situational awareness,” in Proc. Advanced Maui Optical and Space SurveillanceTechnol. Conf. (AMOS), 2017.

[34] S.Riepl, A.Böer, R.Dassing,U.Hessels, J.Eckl, A.Leidig, R.Motz, S.Mähler, C.Schade, M.Schönberger, T.Schüler, “First results from the satellite observing system Wettzell”, 19th International Workshop on Laser Ranging, October 27-31, 2014.

[35] G. Fasano, D., Accardo, A. Moccia, and D. Morone, “Sense and avoid for unmanned aircraft systems”. IEEE Aerospace and Electronic Systems Magazine, 31(11):82–110, 2016.

[36] A. Sedunov et al “Passive acoustic system for tracking low-flying aircraft”, IET Radar, Sonar & Navigation, 2016.

[37] Standardized European Rules of the Air (SERA), “Commission Implementing Regulation (EU) No. 923/2012” https://eur-lex.europa.eu/legal-content/EN/TXT/PDF/?uri=CELEX:02012R0923-20220127&from=EN

[38] Kashiyama T, Sobue H, Sekimoto Y. Sky Monitoring System for Flying Object Detection Using 4K Resolution Camera. Sensors (Basel), 2020.

[39] Wu, Sijie, Kai Zhang, Shaoyi Li, and Jie Yan. 2020. "Learning to Track Aircraft in Infrared Imagery" Remote Sensing 12, no. 23: 3995.

[40] J. Canny, "A Computational Approach to Edge Detection," in IEEE Transactions on Pattern Analysis and Machine Intelligence, vol. PAMI-8, no. 6, pp. 679-698, Nov. 1986.

[41] Satoshi Suzuki, Keiichi Abe, Topological structural analysis of digitized binary images by border following, Computer Vision, Graphics, and Image Processing, Volume 30, Issue 1, 1985.

[42] Duda, R.O.; Hart, P.E. (January 1972). “Use of the Hough Transformation to Detect Lines and Curves in Pictures”